Proceedings of the 21st ICSMGE, Vienna, Austria, 14 – 19 June 2026. Pistrol, Adam & Schweiger (eds.)
Published by: ÖGG, Austrian Society for Geomechanics, Salzburg, Austria, ISBN 978-3-9503898-4-5
https://doi.org/10.53243/ICSMGE2026-2117

Comparative study of the liquefaction behavior of three coastal sands in Peru

Guillermo J. Zavala, Dennys J. Taipe, Franklin R. Olaya
Department of Engineering, Pontificia Universidad Católica del Perú, Lima, Perú, gzavala@pucp.edu.pe

Miguel A. Pando
Department of Civil, Architectural and Environmental Engineering, Drexel University, Philadelphia, USA.

ABSTRACT: This study investigates the liquefaction behavior sands from Canchamaná (CM), Paracas (PA) and Tambo de Mora (TM) coastal sites located in the Ica region of Peru. All sites have experienced extensive earthquake damage after significant earthquakes. This comparative study assesses the influence of differences in their depositional history, grain sizes, mineralogical compositions, and grain morphology on their liquefaction susceptibility. The test program involved determination of index properties, grain size distribution, mineralogy, and particle morphology. The three sands are fine poorly graded (SP) sands with subrounded to subangular grains, and all have a mixed mineralogy containing quartz, feldspars and other minerals. The liquefaction susceptibility of the three test sands was assessed with a comprehensive set of undrained cyclic triaxial tests performed on samples prepared at loose and medium-dense relative densities, under confining stresses of 100 kPa and 200 kPa. Results show that in a loose condition at 100 kPa confining stress, PA sand (more rounded particles) shows the highest cyclic resistance ratios (CRR), followed by TM and CM sands, while at 200 kPa, loose TM sand (more angular particles) shows the highest resistance, because PA sand is the most affected by the confining stress change. For medium-dense specimens, TM sand shows the greatest CRR under a confining stress of 100 kPa, followed by PA and CM sands. However, at 200 kPa confining stress, the cyclic resistance of PA and CM sands remains relatively unchanged, while TM sand exhibits a marked reduction, becoming the least resistant of the three. Summarizing, the CRR of the sands changes with confining stress, but this change depends on the relative density. In addition, the cyclic resistance increases with increasing coefficient of uniformity. The differences observed show the critical role of considering particle-scale properties and mineralogy in the characterization of the macroscopic cyclic behavior and liquefaction susceptibility of sands.

KEYWORDS: Cyclic resistance ratio, coefficient of uniformity, particle-scale properties, mineralogy, Peruvian coastal sands.

1 INTRODUCTION

Liquefaction is commonly observed in loose, saturated sandy soils subjected to strong earthquakes or dynamic vibrations. Liquefaction manifests as a drastic reduction in shear strength and stiffness of soils, resulting from a rapid rise in pore water pressure during cyclic loading. When pore pressure increases sufficiently, the soil effectively loses its structural integrity and behaves similar to a viscous liquid, thus the term "liquefaction". Consequences of soil liquefaction include ground subsidence, settlement, sand boils, lateral spreading, slope instability, and structural damage or collapse.

Assessment of liquefaction potential typically relies on empirical data derived from post-earthquake observations and field testing at documented liquefaction sites. Seed and Idriss (1971) established foundational methodologies still widely used in practice. Their work presented a comprehensive database of case histories from various sites, predominantly involving siliceous sands (e.g. Ottawa sand, Toyoura sand, Monterey sand). In contrast, the liquefaction susceptibility of coastal sands (which often have a mixed mineralogy) have not been received the same level of attention.

Undrained cyclic triaxial tests are popular to study the liquefaction potential of sands (Seed & Lee 1966, Seed & Idriss 1971, Ishihara 1993, Youd et al. 2001, Idriss & Boulanger 2008, and NASEM 2021). Table 1 summarizes relevant experimental studies of sand liquefaction using undrained cyclic triaxial tests and includes information on key parameters such as relative density (D_r), effective consolidation stress (σ'_{3cons}), cyclic stress ratio (CSR), frequency of cyclic loading application (f), specimen preparation methods, average particle size (D_{50}), and fines content. CSR is defined as the amplitude of applied cyclic shear stress divided by the initial effective confining stress.

As shown in Table 1, most studies used CSR values ranging from 0.1 to 0.35. However, some studies used CSR values as high as 0.70 (e.g., Chien et al. 2002). D_r typically ranged between 30% and 75%. All the studies listed in this table employed isotropically consolidated specimens with varying confinement pressures, ranging from 50 to 400 kPa.

Table 1. Selected experimental liquefaction studies using CU cyclic triaxial tests (adapted from Sandoval and Pando 2012).

Reference	Test Sand	D_{50} (mm)	D_r (%)	σ'_{3cons} (kPa)	Sample preparation	CSR range	f (Hz)	Fines (%)
Seed & Lee (1966)	Clean Sacramento River sand	0.22	38 76	100	N/A	0.26 – 0.57	2.0	0
Silver et al. (1976)	Monterey # 0 sand	0.36	60	100	Moist tamping	0.14 – 0.29	1.0	0
Horita (1985)	Monterey # 0/30 sand	0.45	30	200	N/A	0.28, 037	0.5	N/A
Anwar (1989)	Monterey # 16 sand and Coarse Monterey sand	1.35 3.0	45 55 60	200	Moist tamping	0.20 – 0.35	0.10	N/A
Erten (1994)	Ottawa # 20–30 sand	0.73	50 70	100	N/A	0.15, 0.40	1.0	0, 10, 20, 30, 60
Amini (2000)	Ottawa # 20-30 sand	0.73	40	50 100 250	Moist tamping and wet pluviation	0.05, 0.25	N/A	10, 30, 40, 50
Nguyen (2002)	Nevada sand and Lone sand	0.14 0.20	8.5 35	400	N/A	0.11 – 0.28	0.03 1.0	N/A
Chien et al. (2002)	Taiwanese soils	0.22 029	35 55 75	N/A	Moist tamping	0.25 – 0.70	N/A	0, 5, 10, 20, 30
Genduso (2005)	Manufactured medium SP sand	0.55	60	50 100 200	N/A	0.1, 0.2, 0.3, 0.4, 0.5	0.05	N/A
Ghionna & Porcino (2006)	Coarse Gioia Tauro sand	2.0	42	40	Air pluviation and water sedimentation	0.11 – 0.44	0.20	N/A

Notes: N/A= no information reported; D_r= relative density; f= frequency of harmonic cyclic loading D_{50}= mean particle size; σ'_{3cons}= isotropic effective consolidation stress; CSR= cyclic stress ratio.

Coastal sands differ significantly from terrigenous or alluvial sands in geology, mineralogy, and depositional environment. These differences commonly lead to distinct index and physical properties, such as grain size distribution, particle shape, mineralogy, and specific gravity, which in turn can influence their liquefaction susceptibility, when compared to tests on terrigenous siliceous sands tested under similar conditions and at similar initial states (e.g., relative density and consolidation stress). For this reason, the authors believe there

is strong merit in investigating the response of Peruvian coastal sands and comparing their undrained cyclic behavior with that of the more commonly studied terrigenous siliceous sands.

This paper presents a comparative study that investigates differences in liquefaction susceptibility of three Peruvian coastal sands considering differences in index properties, geology and depositional history, mineralogical compositions, and particle morphology. The liquefaction susceptibility study involved cyclic triaxial tests performed on specimens prepared at loose and medium dense relative densities and isotropic consolidation stress levels of 100 and 200 kPa.

2 TEST SAND MATERIALS

The specimens of coastal sands evaluated in this study were retrieved from the west coast of Perú at the locations detailed in Table 2. The sands are referred to as Paracas (PA), Canchamaná (CM) and Tambo de Mora (TM). The sand samples were retrieved from shallow depths up to approximately 0.70 m.

Table 2. Sampling site information for test sands

Location	Sample ID	Latitude	Longitude	Sampling depth (m)	Ground Water level(m)
Canchamaná	CM	13°26'22.34"S	76°10'53.72"W	0.3-0.5	Not found
Paracas	PA	13°50'30.35"S	76°15'20.09"W	0.5-0.7	Not found
Tambo de Mora	TM	13°27'23.44"S	76°10'58.74"W	0.3-0.5	0.3

All sands were in an uncemented state. Grain size distribution curves for the three sands along with "standard" sands for comparison are shown in Figure 1. This figure shows that TM sand is the coarsest, followed by CM sand and then PA sand, which is the finest. These sands have a wider range of particle sizes than Toyoura sand (Yang & Sze, 2011) and Ottawa #20-30 sand (Sandoval & Pando, 2012), all of them being coarser than Toyoura sand but finer than Ottawa #20-30 sand.

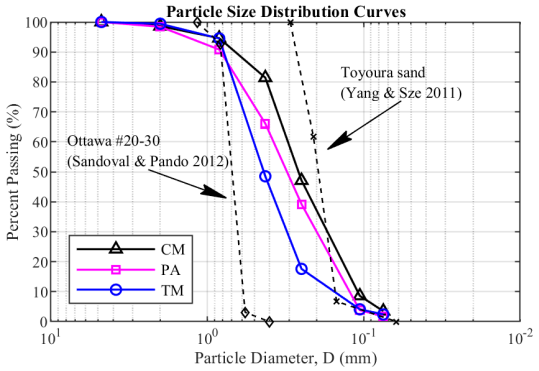

Figure 1. Grain size distribution of the three tests sands

The main index properties of the three sands are listed in Table 3. The gradation curves are different but poorly graded with coefficient of uniformity values of 2.82, 3.25 and 3.4, for the CM, PA, and TM sands respectively. The mean particle size (D_{50}) of the three sands ranges from 0.26 mm (CM) to 0.44 mm (TM). All test sands are uncemented and classify as poorly graded sands (SP) with less than 5% fines (particles <#200). It is noted that the coefficient of uniformity (C_u) for TM and PA sands is similar, but it is notably lower for CM sand. The particle shapes of the three test sands are from subrounded to subangular. Binarized microscope photographs of particles between sieves #40 and #60, in which the D_{50} of the three sands lay, are shown in Figure 2. In these photographs, it can be qualitatively observed that TM and CM sands exhibit less roundness compared to PA sand, which appears to have the most rounded particles. Roundness is quantified as the average radius of curvature of surface features relative to the radius of the maximum sphere that can be inscribed in the particle Krumbein and Sloss (1963).

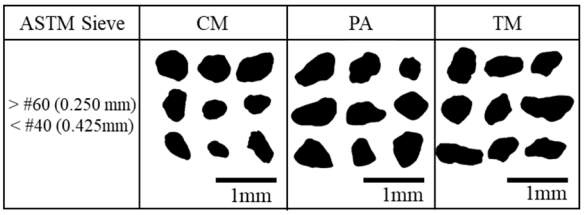

Figure 2. Micrographs of test sands for binarized particles between #60 and #40 sieves.

Table 3. Summary of main index properties for Peruvian test sands used in this study

Parameter	CM	PA	TM	Ottawa Sand #20-30	Toyoura sand	ASTM Standard
USCS	SP	SP	SP	SP	SP	D2487
D_{10}, mm	0.11	0.12	0.15	0.65	0.16	
D_{30}, mm	0.17	0.20	0.31	0.71	0.19	
D_{50}, mm	0.26	0.32	0.44	0.75	0.22	
D_{60}, mm	0.31	0.39	0.51	0.78	0.23	D422 D463
C_u	2.82	3.25	3.40	2.10	1.392	
C_c	0.85	0.85	1.26	1.10	0.961	
Fines content, %	1.80	3.50	2.40	0.00	0.00	
Gs	2.74	2.66	2.90	2.65	2.64	D485
$\gamma_{d\ min}$, kN/m^3	14.9	15.1	14.70	14.6	13.1	D4254
e_{max}	0.80	0.73	0.93	0.78	0.977	
$\gamma_{d\ max}$, kN/m^3	18.4	18.1	18.5	17.3	16.1	D4253

Figure 3 shows X-ray diffraction (XRD) tests results showing the main mineral components. The XRD results show that the predominant mineral group is feldspars with 55%, 52%, and 49% for the CM, PA, TM sands, respectively. The second mineral is quartz with 36%, 27%, and 24% for the PA, TM, and CM sands, respectively.

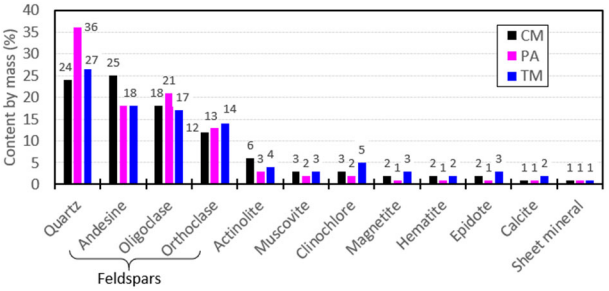

Figure 3. X-ray diffraction results for the three test sands.

As shown in Table 3, the specific gravity of the CM, PA and TM sands are 2.74, 2.66, 2.90, respectively. These specific gravity values correspond to bulk samples and are close to computed weighted average specific gravity values considering the mineralogic compositions of the three sands shown in Figure 3 and the typical specific gravity values of the different pure mineral components.

A summary description for each sand is provided below:

- Canchamaná Sand (CM): Uncemented, fine to medium grained, yellow to brown in color, with sub-angular to angular grains, poorly graded mixed mineralogy SP sand. The mean particle size D_{50} is 0.26 mm, and the coefficient

of uniformity C_u is 2.82. This sand is composed mainly of feldspars (55%) followed by quartz (24%). This sand was qualitatively assessed as having the intermediate roundness of particle compared to the other test sands.

- Paracas Sand (PA): Uncemented, fine to medium grained, yellow to brown in color, with sub-rounded to sub-angular grains, poorly graded mixed mineralogy SP sand. The mean particle size D_{50} is 0.32 mm with a C_u of 3.25. This sand is composed mainly of feldspars (52%) followed by quartz (36%). The PA sand had the highest quartz content of the three test sands and is qualitatively assessed as having the more rounded particle shape of the of the three sands.
- Tambo de Mora Sand (TM): Uncemented, fine to medium grained, gray to black in color, with sub-angular to angular grains, poorly graded SP mixed mineralogy sand. The mean particle size D_{50} is 0.44 mm with C_u of 3.40. This sand is composed mainly of feldspars (49%) followed by quartz (27%). This sand was found to have the least rounded particle, and the highest specific gravity and coefficient of uniformity as compared to the other test sands.

3 EXPERIMENTAL PROGRAM

The cyclic triaxial tests for the three sands were carried out using a GDS Enterprise Dynamic Triaxial Testing System (ELDYN) automatic cyclic triaxial equipment at the Soil Mechanics Laboratory of the Pontificia Universidad Católica del Perú (PUCP). For the sake of brevity, and since frequency has been reported by many as not a major factor in CSR vs N plots, we only present results for a frequency of 0.1 Hz.

Specimens, approximately 100 mm in height and 50 mm in diameter, were prepared using the "dry tamping" technique with five layers and the under-compaction method suggested by Ladd (1978). The initial relative densities of the specimens, prior to saturation and consolidation, ranged from 15% to 50%.

Table 4 shows the initial test conditions considered in this study, which include two initial relative densities and two effective confining stresses. The values of relative density shown were calculated after the consolidation stage.

Table 4. Test matrix for undrained cyclic triaxial (CTX) tests.

Data set ID	Sand	No of tests	Sample Initial State				
			Relative density D_r (%)			σ'_{3cons} (kPa)	
			Description	Mean	StDev	Mean	StDev
1	PA	12	Loose	24.8	5.7	99.1	2.5
2		11	Loose	26.8	4	198.4	0.8
3		6	Med. dense.	56.6	2.5	98.8	0.8
4		12	Med. dense	58	2.2	199.6	1.6
5	CM	13	Loose	26.6	4.9	199.7	1.6
6		7	Loose	34.6	4.2	200.6	0.8
7		6	Med. dense	64.4	1.8	98.3	1.7
8		6	Med. dense	62.1	2.8	198.6	1
9	TM	10	Loose	30.6	3.8	99.7	2.5
10		21	Loose	39.3	3.6	199.9	1.2
11		8	Med. dense	64.8	1.5	98.9	0.6
12		7	Med. dense	61.6	3.2	200	2.5

The results enabled a comparative evaluation of the cyclic resistance ratio (CRR) of the three sands. Specimens were saturated until a Skempton B-values greater than 0.95 were achieved. After saturation, specimens were isotropically consolidated to two different effective stress levels (100 and 200 kPa). The soil specimens experienced densification during isotropic consolidation, which resulted in loose (L) and medium-dense (MD) specimens, with end initial relative densities of approximately 30% and 60%. After the consolidation stress was applied, specimens were allowed to stabilize under this stress for at least 20 minutes prior to the initiation of the undrained cyclic loading phase.

All isotropically consolidated specimens were subjected to uniform sinusoidal stress-controlled undrained cyclic triaxial tests at a frequency of 0.1 Hz, and Cyclic Stress Ratio (CSR) values between 0.1 and 0.25. Typical sets of results are shown in Figure 4, which shows a four-way plot representing the measurement of deviatoric stress, mean effective stress, and axial strain as a function of the number of cycles during the test until reaching initial liquefaction, defined by an excess pore water pressure ratio (r_u) equal or close to 1. This figure shows that, for test series with samples at medium-dense initial relative density and a confining stress of 200 kPa, and loaded at a CSR of 0.21, PA sand requires a larger number of cycles to reach liquefaction compared to CM and TM sands, which exhibit similar behavior in terms of pore pressure generation, axial strain development, stress path evolution and hysteretic loops. This suggests that for this confinement stress and density, the CRR curves for CM and TM should be close together, while the CRR curve for PA will have higher values.

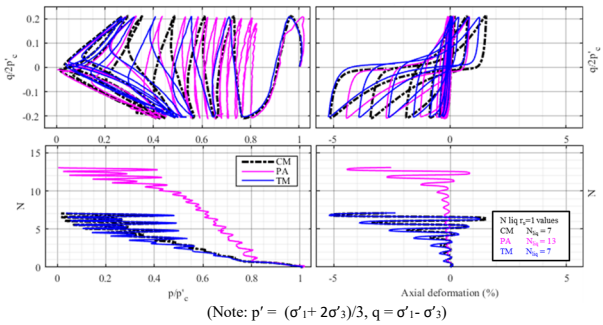

(Note: $p' = (\sigma'_1 + 2\sigma'_3)/3$, $q = \sigma'_1 - \sigma'_3$)

Figure 4. Typical four-way plot of triaxial cyclic test on 3 sands for medium dense sands Dr ≈ 60%, CSR = 0.21, and 200 kPa confining stress.

4 RESULTS AND DISCUSSION

Liquefaction susceptibility of the three sands was also assessed by evaluating curves of CRR versus cycles to reach liquefaction. Figure 5 shows CRR curves for the PA sand in a loose state, for two effective confining pressures: 100 kPa and 200 kPa. Each point represents the number of cycles at a specific CSR that caused initial liquefaction.

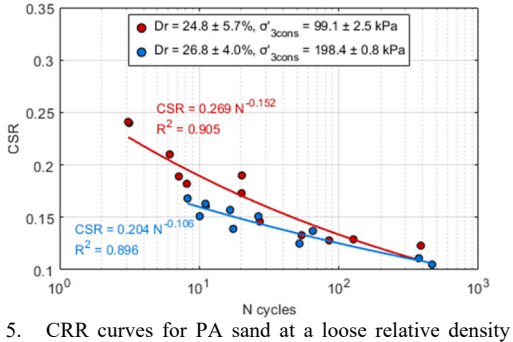

Figure 5. CRR curves for PA sand at a loose relative density and isotropic consolidation stresses of 100 kPa and 200 kPa.

The CRR curves for the PA follow these general trends: i) an increasing number of cycles to liquefaction with decreasing applied CSR, and ii) the CRR values are lower at 200 kPa confinement compared to 100 kPa, showing that increased confining stress tends to make sands more contractive, leading to a reduction in their cyclic resistance.

Figure 6 presents results of the CRR curves for PA, CM, and TM sands for confining stresses of 100 kPa (Figure 6a) and 200 kPa (Figure 6b). Two average relative densities are shown for each sand, 30% and 60%.

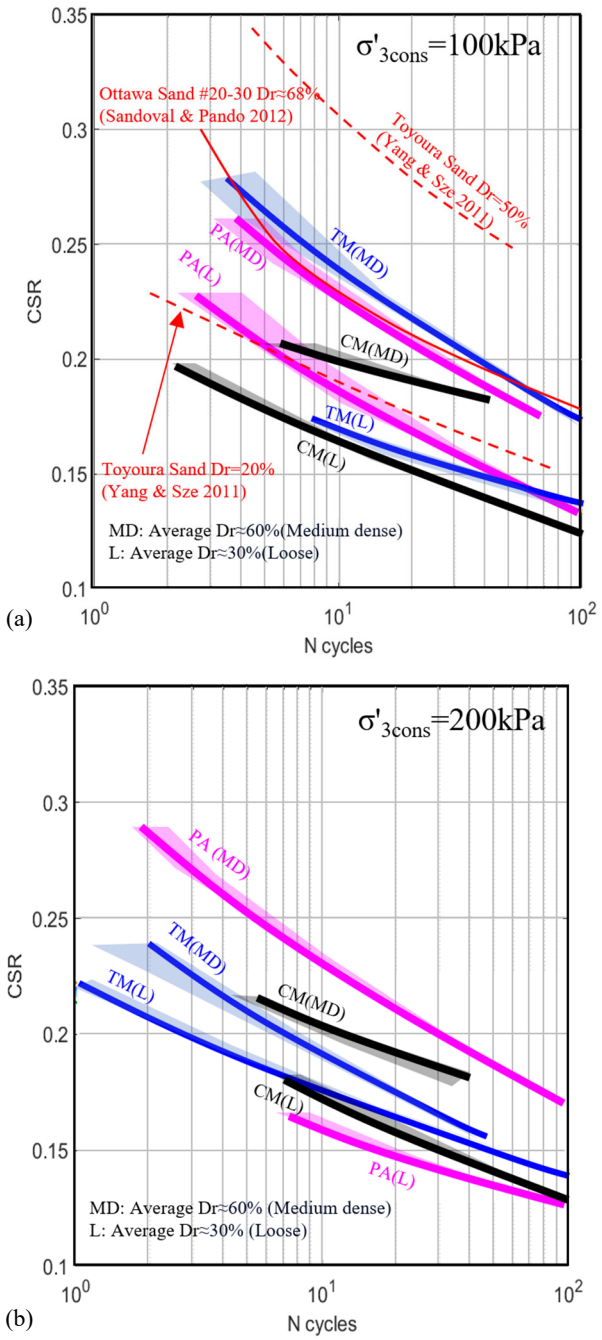

Figure 6. Cyclic Resistance Ratio (CRR) curves for the CM, PA, and TM sands for confining stress of (a) 100 kPa, and (b) 200 kPa.

Figure 6a shows that for tests with an initial effective confining stress of 100 kPa and loose Dr, the CM sand has the smallest CRR values, followed by TM and PA sands. An increase in relative density for the three sands leads to an increment in the CRR curves. However, the CRR curves from cyclic triaxial tests at 100 kPa and medium dense sands shows that the TM sand exhibits a greater increase in CRR when moving from a loose to a medium-dense state at this confining stress, which leads to TM sand having the highest cyclic resistance of the three test sands in this latter state, closely followed by PA sand. Both sands have CRR curves that are similar to the one reported by Sandoval and Pando (2012) for 20-30 Ottawa sand tested at the same confining stress level and at medium dense condition. The higher CRR of the TM sand at the medium dense Dr and 100 kPa confinement stress may be attributed to its more angular particles. Santamarina et al. (2001) reported that the normal stiffness of the particle skeleton at small deformations is fundamentally determined by particle contacts. A denser packing with more angular particle shapes, promotes more stable and effective contact points, leading to higher resistance. The CRR curve for the TM may also be related to its higher coefficient of uniformity (C_u) that is in line with findings reported by Rehman et al. (2025), where higher coefficient of uniformity leads to higher cyclic resistance ratios. In comparison, the mean CRR curves of Toyoura sand and Ottawa #20-30 sand are higher than those of the test sands in a medium-dense state at 100 kPa confining stress. This indicates that the test sands possess a lower cyclic resistance than those reference sands.

Figure 6b summarizes CRR curves obtained for cyclic triaxial tests performed at an effective confining stress of 200 kPa. The results for the three sands prepared at a loose Dr, show that the CRR curves for the three test sands are very similar with the TM having the highest CRR curves, closely followed by CM and PA sands. For this level of confinement stress CRR curves for all three sands show an increase with increasing relative density. The TM sand only shows a slight increase in CRR with an increase of relative density, that is smaller relative to the observed increase at 100 kPa. In turn, CM sand, and more notably PA sand, show a more substantial increase in CRR with relative density. For 200 kPa initial confinement and a medium dense Dr the CRR curves from highest to lowest correspond to the PA sand, followed by CM sand and TM sand. In summary, Figure 6 indicates that all CRR curves increase with increasing relative density for a particular effective stress level. This expected behavior reflects the improved particle interlocking and reduced void ratio in denser states. However, the relative position of the CRR curves for the three test sands varies for the different initial states considered thus depending on the relative density and confining stress.

Figure 7 shows a comparison of the CRR curves for the two relative density levels considered of loose and medium-dense states. Although the cyclic shear stress level required to reach liquefaction at a certain number of cycles increases with confining pressure, the cyclic stress ratio (CRR) typically decreases with increasing confining pressure. The results for loose sands shown in Figure 7a show that only the PA sand followed this typical trend reported in the literature. In contrast the TM and CM sand showed negligible decrease of CRR with increasing effective stress. For Figure 7b, that summarizes results from tests performed on samples prepared at a medium dense Dr, only TM sand results showed a clear decrease of CRR curves with increasing effective stress, compared to PA and CM sands, which show negligible decrease of CRR with increasing effective stress.

The CRR curves are a function of the initial state of the sample defined by density and confining stress; but also depend on the relative position to its critical state line, and on particle-scale properties and minerals.

As mentioned before, the normal stiffness of the particle skeleton at small deformations (macro-scale behavior) is related to the microstructural geometry and number of particle contacts

(Santamarina et al. 2001). The influence of these factors can be further related to changes (increase or decrease) in initial density and effective confining pressure, leading to the observed differences in cyclic resistance and sensitivity among CM, PA, and TM sands.

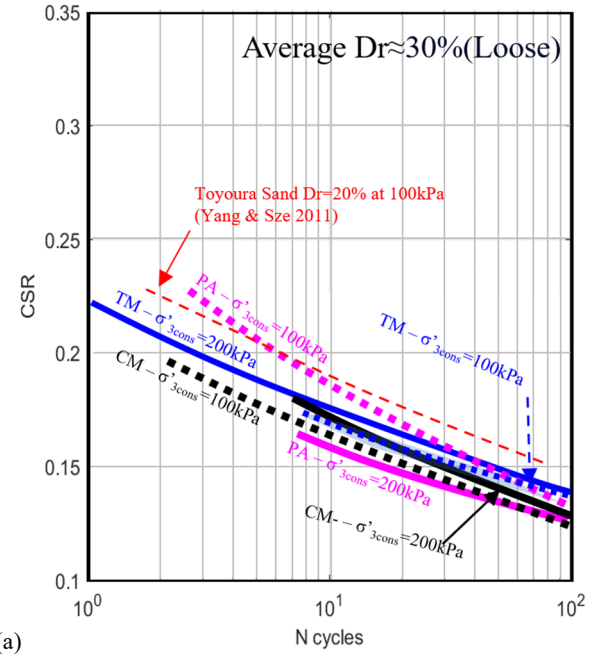

(a)

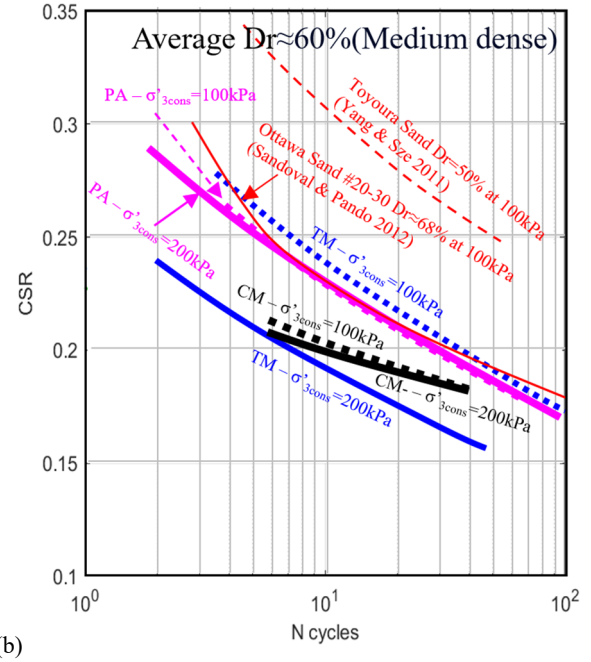

(b)

Figure 7. Cyclic Resistance Ratio (CRR) curves for the PA, TM, and CM sands for average relative density of (a) 30%, and (b) 60%.

The important influence of particle-scale properties on soil behavior including liquefaction resistance has been highlighted by Santamarina et al. (2001) and Ashmawy et al. (2003). The later study reports that particle shape controls the distribution of internal forces within a soil skeleton. For example, sands with rounded particles, such as Ottawa sand, will generate larger contact forces that concentrate into distinct "force chains," which leads to a highly contractive response and rapid liquefaction. In contrast, angular particles distribute smaller contact forces more uniformly across the assembly, creating a more stable fabric and exhibiting a dilative response under cyclic loading. However, the formation of this resistant fabric and the contact surfaces is not solely dependent on particle shape. The process is also a function of the coefficient of uniformity (C_u), relative density (Dr), and confining stress (σ'_{3cons}). The combination of a well-graded soil (high C_u), greater compactness (high Dr), and elevated effective confining stresses directly influence how inter-particle contacts are established. This, in turn, defines the soils ultimate cyclic resistance to liquefaction. In essence, resistance is the result of the interaction between particle geometry and the consolidation and compaction conditions.

The influence of the coefficient of uniformity (C_u) was reported by Rehman et al. (2025). Figure 8 shows data compiled from several authors, which indicate a relationship between the CRR at N=15 (CSR required to reach liquefaction in 15 cycles) and the coefficient of uniformity (C_u). Although the data in Figure 8 shows significant scatter, it shows that the CRR-15 increases with increasing C_u. Figure 8 also shows the results obtained from the three sands tested in this study which tend to agree with the trend found by Rehman et al. (2025).

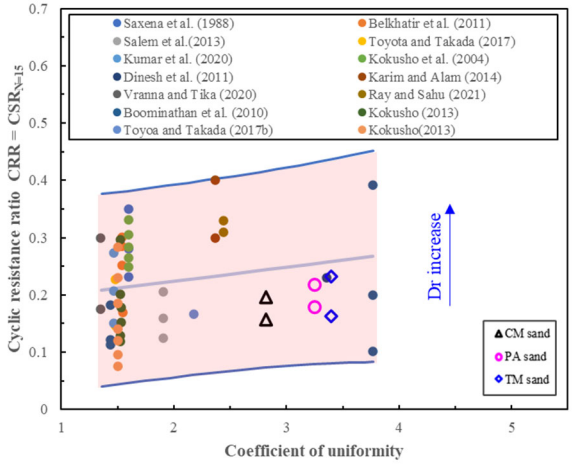

Figure 8. Variation of cyclic resistance ratio CRR with coefficient of uniformity (σ'_{3cons}=100 kPa) (adapted from Rehman et al. 2025).

The behavior outlined by Rehman et al. (2025) is linked to soil gradation. A higher C_u indicates a wider range of particle sizes, which facilitates more effective particle interlocking. This improved interlock, in turn, enhances the cyclic shear resistance of the soil (expressed in terms of CRR-15).

It is also important to note the coupled effect of Dr and C_u. The vertical arrow on the plot highlights that cyclic resistance increases with Dr, demonstrating that cyclic resistance is influenced by particle size distribution, soil relative density, and confinement pressure. While the data shows a marginal CRR variation for $C_u \geq 4$, the combined effect of a well-graded and denser soil is clearly evident in this study.

5 CONCLUSIONS

The liquefaction behavior of three sands from coastal Peru sites, Canchamaná (CM), Paracas (PA), and Tambo de Mora (TM) was evaluated experimentally by comparing the CRR curves obtained from a comprehensive cyclic triaxial test experimental program. This evaluation was conducted for two initial relative densities (loose at D_r=30% and medium dense at D_r=60%) and for two levels of confining stress (100 and 200 kPa).

Specific observations from CM, PA, and TM properties and cyclic resistance indicate the following:

The three sands are fine poorly graded clean sands and with reasonably close grain size distribution curves. Based on the mean particle size, the TM is the coarsest sand, followed by PA and CM sands. The coefficient of uniformity (C_u) of the CM sand is the lowest among the three, whereas TM and PA sands have similar slightly higher values. All test sands had particle that ranged from subrounded to subangular. Qualitatively, the PA sand showed the more rounded grains with decreasing roundness for the CM sand followed by TM sand. All test sands had mixed mineralogy. The predominant mineral group for three test sands was feldspars with 55%, 52%, and 49% for the CM, PA, TM sands, respectively. The second mineral was quartz with 36%, 27%, and 24% for the PA, TM, and CM sands, respectively.

The CRR vs N curves for specimens prepared at a loose state at 100 kPa of effective confining stress, the PA sand showed the highest cyclic resistance, followed by the TM and CM sands. The results for cyclic CU triaxials at a confining pressure of 200 kPa, and prepared to a loose relative density, showed the TM had the highest resistance, followed by the CM and PA sands. Toyoura and Ottawa sands showed higher cyclic resistance than the three sands of this study at both the loose and medium states at 100 kPa of effective confining stress.

In this paper the particle shapes are described qualitatively based microscope images and the CSL were not evaluated. A preliminary hypothesis to explain, for example, the slight decrease of the cyclic resistance of the TM sand when the confinement was increased from 100 to 200 kPa, is that its more angular particles compared to the other two test sands developed more interlocking at higher stress levels thus higher particle contact stresses could be a dominant factor in increasing the liquefaction resistance. This observation is being investigated by the authors in the ongoing study.

For medium-dense specimens at 100 kPa confinement, TM sand again displays higher resistance. Yet, at 200 kPa confinement in the medium-dense condition, TM shows a significant decrease in cyclic resistance, and PA sand becomes the most resistant sand. The preliminary hypothesis to explain the slight decrease of the cyclic resistance of the PA sand when the confinement was increases from 100 to 200 kPa is that the higher effective confining stress at this density state greatly increases the normal forces across its more numerous making friction at these contacts the primary resistance mechanism. CM sand behavior often falls between PA sand and TM sand, showing distinct trends in its slope and sensitivity depending on the density and confinement.

The differences in liquefaction resistance expressed in terms of CRR values to reach liquefaction in 15 cycles (CRR_{15}) in terms of differences of the coefficient of uniformity C_u as reported by Rehman et al. (2025) was also investigated for the three test sands. The observed general trend was that CRR_{15} increased with increasing coefficient of uniformity. However, test sand TM with the highest C_u value was found to have a lower CRR_{15} than test sand PA.

The effect of particle shape and mineralogy on cyclic resistance has to be investigated further. Although all test sands had quartz contents of at least 24%, there were important amounts of other minerals that have different mineral friction angles. Regarding particle shape, the PA test sand with the most subrounded particles had important differences in results compared to the TM sand with the more angular particles. The role of particle morphology in particle contacts and interlocking has to be investigated further. However, the differences observed show the critical role of particle-scale properties and mineral can have in predicting the macroscopic cyclic behavior of coastal sands.

6 ACKNOWLEDGEMENTS

The authors would like to thank the Department of Engineering at Pontificia Universidad Católica del Peru for providing funding to perform the research, and the staff technicians at the Soil Mechanics Laboratory of the Pontificia Universidad Católica del Peru for their invaluable help in running the tests for this study. The authors also extend their appreciation to the District Municipality of Tambo de Mora, for aiding and authorizing the extraction of sand samples from local sites, thereby enabling the acquisition of representative materials necessary for the dynamic testing program of this study.

7 REFERENCES

Ashmawy, A., Elsheshtawy, M., & El-Sherbiny, H. (2003). Evaluating the Influence of Particle Shape on Liquefaction Behavior Using Discrete Element Modeling.

Chien, L.-K., Oh, Y.-N., & Chang, C.-H. (2002). Effects of fines content on liquefaction strength and dynamic settlement of reclaimed soil. *Canadian Geotechnical Journal*, 39(1), 1–13. https://doi.org/10.1139/t01-083

Idriss, I. M., & Boulanger, R. W. (2008). *Soil liquefaction during earthquakes.* Earthquake Engineering Research Institute.

Ishihara, K. (1993). Liquefaction and flow failure of sand deposits. *Géotechnique*, 43(3), 353-410.

Krumbein, W. C., & Sloss, L. L. (1963). *Stratigraphy and sedimentation* (2nd ed.). Freeman and Company.

Ladd, R. S. (1978). Preparing test specimens using undercompaction. *Geotechnical Testing Journal*, 1(1), 16–23.

NASEM (National Academies of Sciences, Engineering, and Medicine). (2021). *State of the art and practice in the assessment of earthquake-induced soil liquefaction and its consequences.* https://nap.nationalacademies.org/23474..

Nguyen, T. Q. (2002). Sand Behavior from Anisotropic and Isotropic Static and Dynamic Triaxial Tests. (PhD Thesis). University of Nevada, Reno.

Rehman, M. U., Kandasami, R. K., & Banerjee, S. (2025). *Simplified approach for liquefaction assessment in granular soils: integrating bulk and grain properties*. Springer Nature. https://doi.org/10.1007/s10035-025-01529-4

Sandoval, E., & Pando, M. A. (2012). Experimental assessment of the liquefaction resistance of calcareous biogenous sands. *Earth Sciences Research Journal*, 16(1), 55–63.

Santamarina, J. C., Klein, K.A. & Fam, M.A. (2001). S*oils and waves: Particulate materials behavior, characterization and process monitoring*. Wiley. https://doi.org/10.1007/BF02987719

Seed, H. B., & Idriss, I. M. (1971). Simplified Procedure for Evaluating Soil Liquefaction Potential. *Journal of the Soil Mechanics and Foundations Division*, 97(9), 1249-1273. https://doi.org/10.1061/JSFEAQ.0001662

Seed, H. B., & Lee, K. L. (1966). Liquefaction of saturated sands during cyclic loading. *Journal of the Soil Mechanics and Foundation Division*, 92(3), 25-58.

Skempton, A. W. (1954). The pore pressure coefficients A and B. *Géotechnique*, 4, 143–147.

Yang, J., & Sze, H. Y. (2011). Cyclic behaviour and resistance of saturated sand under non-symmetrical loading conditions. *Géotechnique*, 61(1), 59–73.

Youd, T. L., Idriss, I. M., Andrus, R. D., Castro, G., Christian, J. T., Dobry, R., ... & Tokimatsu, K. (2001). Liquefaction resistance of soils: Summary report from the 1996 NCEER and 1998 NCEER/NSF workshops on evaluation of liquefaction resistance of soils. *Journal of Geotechnical and Geoenvironmental Engineering*, 127(10), 817-833.